Preliminary results about micro scale slope mass movements in black marls

J. Bechet[1], J. Duc[1], M. Jaboyedoff[1], A. Loye[1] and N. Mathys[2]

[1]{University of Lausanne, Risk-group - ISTE - Institute of Earth Sciences, Lausanne, Switzerland}

[2]{ IRSTEA Grenoble, Unité de recherche Erosion Torrentielle, Neige et Avalanches, BP 76, 38402 Saint Martin d'Hères, France }

Correspondence to: M. Jaboyedoff (michel.jaboyedoff@unil.ch)

Abstract

An undisturbed sample of badlands soil (1 m long, 0.5 m wide and 0.15 m thick) has been extracted in situ in order to study with high detail the millimetre scale surface processes caused by natural rainfall. The sample is composed of black-marls soil, coming from a badlands area of Draix Observatory (SE of France).After it thoughtful extraction, the undisturbed sample has been placed with the same slope angle (45°) as it was originally placed in situ. This portion of soil was then monitored by a Leica ScanStation II terrestrial laser scanner (TLS). This experiment allowed identifying several surface processes interpreted as micro-landslides, swelling of the black-marls material and lateral expansion closing desiccation cracks. All these processes have been studied and identified with high detail (millimetre scale accuracy and resolution). These micro-processes are important to gain understanding of soil erosion sources and infiltration as shown by our preliminary observations.

1 Introduction

Small black-marls watersheds have strong responses to climate forcing (Malet et al., 2007). This study aims to better understand the erosional behaviour and the micro-morphological evolution on these materials caused by micro mass-movements as response to precipitation. The goal of this experiment was to extract an undisturbed sample of black marls and expose this material to a natural rainfall event, in order to monitor the sample's surface evolution using a 3D laser scanner. This monitoring has permitted us to study the surface deformation and erosion processes with high detail. The duration of the experiment and the rainfall intensity does not permit to investigate the splash erosion as first intended, because its effect is below the resolution of our acquisition and the rather low intensity of the rainfall, which can be important when rainfall is intense (Selby, 1993).

In the past, several studies of artificial-rain simulations have been performed on the site of the Draix Observatory (ORE Draix), which is an observatory dedicated to the research of mountain hydrology and erosion processes. Previous works focused on the measurement of sediment transport (Oostwood and Ergenzinger, 1998) and runoff in function of precipitations (Mathys et al., 2005). The badland surface ground evolution has already been monitored during rainfall simulations by using a pin-type micro relief-meter and photographies (Torri et al., 1999; Mathys et al., 2005), but these tools were not able to reach the same precision as a laser scanner. Recent studies showed the potentiality of observing and characterizing erosion processes at the level of micro-topography using laser scanner (Schmid et al., 2004; Barneveld et al., 2013).

The soil sample was extracted from the experimental site of Draix (ORE Draix, IRSTEA) in the south of French Alps, a badlands area near the city of Digne-les-Bains. The experiment has been performed in Lausanne (Switzerland), where precipitations can be considered similar to Alpine region. For the monitoring of the sample surface a TLS has been used, in order to:

(1) Identify surface processes at the millimetre scale.

(2) Quantify the swelling of the material in the marls during rainfall events

(3) Map all the possible modifications of the terrain surface

2 Geological settings

The badlands near the village of Draix are composed of weathered black-marls of Middle Jurassic age (Callovo-Oxfordian). This black marl formation is more than 2000 m thick in some places (Antoine *et al*., 1995). The upper 10 cm of the ground is constituted of loose detrital material made of clasts and platelets produced locally (Maquaire et al., 2002). Between the intact rock and this layer, the regolith is usually about 30 cm to 1 m thick (Maquaire et al., 2002; Antoine et al., 1995). The clay size fraction content of the black-marls located in this part of France has been measured at 35±5% (Caris et Van Asch, 1991), but the clay mineral content is of approximately 10%, mainly illite and traces of smectite and interstratified clay minerals (Antoine et al., 1995). During rainfall events water infiltrates the ground and the material can swell because of the fine grain material behaviour and chemical reactions (Antoine et al., 1995). The loose upper layer detrital material is very sensitive to erosion and is a good candidate for experiments of surface processes imaging.

3 Methods

3.1 Samples

The sample of soil used for this experiment was extracted from a marl outcrop with a 45° slope and the bedding crossing the surface of the outcrop close to a perpendicular (Fig. 1a). Nevertheless, the loose detrital material at surface does not display any identifiable bedding structure. The sample is 1 m long, 0.5 m wide and 0.15 m thick. To extract this sample of soil a metal case has been developed to keep undisturbed the soil structure (Figure 1). This was performed by pressing the bottomless box in the ground, tapping with a hammer to slide the bottom plate of the box in order to isolate a sample of the bedrock. This sample has been stored in the laboratory in dry conditions during 3 months before the experiment started, which can be similar to natural conditions.

3.2 Experiment settings

On the 31st May 2011 the soil sample was exposed to a natural rainfall from 11h01 to 17h47. During the experiment the soil sample was located in its extracting metal casing, which has been tilted by 45° in order to get the same inclination as its *in situ* conditions.

The soil sample was scanned every 30 minutes using a ground-based TLS Leica ScanStation II, that produces point-clouds (x,y,z data) in a 3-dimensionnal space (Figure 1c). The direction of the laser pulses line-of-sight and the recorded time-of-flight determine the position of the measured points. The rainfall has been measured by the weather station of the University of Lausanne (PluvioMADD2 from MADD Technology) located at 500 m from the experiment place.

Since the sample was dry at the beginning of the experiment, the sample did not reach full saturation. About 1.3 litres fell on the box during the experiment and most of the rain fall was absorbed by the sediment, which limited the transport of sediment by runoff. We suspect that an small quantity of evaporation may have occurred during the experiment but we did not weight the box before and after the experiment and this minor influence has been neglected in our study.

3.3 Data acquisition

The surface evolution has been monitored for 6 hours 46 minutes by 12 successive laser scan acquisitions. The first scan and the last scan (acquired at 11:01 and 17h47, respectively) have approximatively a point spacing of 0.001 m. All the other scans have a 0.002 m point spacing. From 0 to 50 m, 50% of the laser beam is in a diameter of 4 mm diameter at full width half height (FWHH) (Leica Geosystems AG, 2007). The scan distance was 2 m. The instrument was not moved throughout the experiment, meaning that the position and the orientation of the scan is identical for all of the acquisitions. As a consequence, no scan alignment was necessary to compare the obtained point clouds.

3.4 Data processing

The point clouds were “manually” cleaned from the points that are not imaging the surface of the sample, i.e. the metal casing sides, the background of the scenery and some artefacts, including point away from the terrain’s surface such as rain drops. Only the surface of the sample was kept. Every cleaned scan has a very high point density: more than 400’000 points for the first and last acquisitions and a minimum of 110’000 points for the rest of these scans (Table 1).

Each TLS point cloud was firstly rotated by 45° to obtain on average a horizontal point cloud in order to be able to interpolate in 2.5-dimensions. The interpolations were performed using an inverse distance method with power of 1 (Shepard, 1968) with Surfer 8.0 software (GoldenSoftware). The point clouds were transformed into regular squared grid of 1 mm for the first and last scans and 2 mm for the other datasets. This provided high resolution digital elevation models (DEM) of altitude z above the mean horizontal surface. The search radius for DEM generation was defined in 1.5 times higher than the pixel size, i.e. 1.5 mm for scans with a point spacing of 1 mm and 3 mm for the scans with a point spacing of 2 mm (Figure 2). Although different values of DEM cell size were tested, this value was chosen such as the most adequate compromise between accuracy / resolution. The so generated DEMs were compared to quantify and map surface changes, i.e. mass movements, erosion/deposition processes. Each DEM was subtracted from the initial (or reference) DEM (DeRose et al., 1998). The resulting z difference grids have negative value pixels for the “erosion” and positive value pixels for the “deposit”. To limit the ‘noise’ of the measurements, differences in absolute value inferior to 0.0015 m were ignored; this threshold was obtained by a trial error procedure.

4 Results

The precipitations started at 13h30 and , then it stopped for 30 minutes around 16h00 and then continued up to the end of the experiment. The maximum rainfall intensity (5.2 mm h^{-1}) was reached at 16h30. A cumulated precipitation of 5.5 mm was recorded at the end of the experiment. Three different surface processes of topographic changes were identified and discriminated. The figure 3 displays the difference between the initial and final scans (11h01 and 17h47, respectively). The rising of the surface (z) appears in blue colours and the decrease in z appears in red colours (Figure 3). We considered only the changes that are fully visible in the oblique view of the experiment (box with a slope of 45°).

The micro-topography changes occurred at location 1-2 is shown in Figures 3 and 4. As can be observed in this figure, a depression is formed at the top of a small ridge (in red) and a depression below this ridge is filled in (in blue). This can be interpreted as a downward mass-movement at the millimetre scale. The small particles moved down, filling a desiccation crack. This phenomenon occurred right after the highest intensity rain event, between 17h00 and 17h30 (Figure 5).

When the rain intensity reached 1 mm h^{-1}, the soil started to rise up all over the surface (it means perpendicularly to the surface of the slope at 45°), appearing as a pale blue layer on Figures 3 and 6. This process affecting the entire surface has been measured from 1.5 to 3 mm for the entire experiment, i.e. for a cumulated 5.5 mm of rain (Figure 5). It starts slowly after the first rain. At 16h30 the surface subsided and this process was momentarily slowed down. After that, the processes re-accelerated following the new peak in rain intensity (Figure 5). Note that no significant rise of the topographic surface has occurred at the top of the sample, which was protected from the rain (Figure 3).

Another observed process is linked to changes of the soil surface by lateral expansion (Figures 6 and 7). This process has been observed continuously through the closing of the desiccation cracks, which were present at the surface of the sample.

The last observed process was the stripping of soil particles by the kinetic energy of the raindrops. Although these changes were observed by the authors during the experiment. Unfortunately its magnitude was too small to be significantly monitored by the utilised TLS.

5 Discussion and conclusions

The geometric changes observed at location 1-2 (Figures 3 and 4) occurred almost instantaneously, which excludes rain splashing process, they were interpreted as a micro-landslide. In addition, the two profiles before and after the occurrence of changes mimic the profile change usually observed in real landslides. Such process can be related to the initiation of miniature debris flows (MDFs) observed by Oostwoud and Ergenzinger (1998), but the latter needed heavy rainfall to be transformed in MDFs.

The observed rise of the surface, which reacts fully with a 30 minutes delay with rainfall, is certainly linked to swelling of the material. The soil sample experienced swelling after the first intensity peak, contraction 30 minutes after the stop of rainfall and new rising of the topographic surface once the rain started again. This measured cyclic behaviour demonstrates that swelling and contraction of the soil surface is a reversible process. We can assume that such process is linked to the moderate rainfall intensity, which allows the water to infiltrate and swell part of the fine grain material. Furthermore, this process is not necessarily caused by clay minerals, since they are present in small quantity (mostly illite) in the study area (Antoine et al., 1995). The swelling must dissipate rapidly because of the diffusion of water when the rainfall stops, leading to a decrease of the water effect.

The lateral expansion of the surface within cracks is also certainly linked to swelling, but does not retreat when the rain stops. It is clear from the figures 6 and 7 that the material has expanded. But it is not affected by transport, since no deposit was observed at the bottom. We do not find any definitive explanation for this difference with the rising up process, but it must be related to gravity which increases the effect of swelling downward. Then when both sides of the crack touch each other the moisten zone doubles its thickness, decreasing the diffusion effect. In addition, such processes must be part of the creeping (Selby, 1993), because probably the retreat by drying will be less effective for the downward part, leading to slow progressive movements downward.

The above interpretations are also important for the understanding of the infiltration process. It is clear that cracks play an important role in the infiltration rates (Mitchell and van Genuchten, 1993) and subsequently for the destabilisation of slopes (Stumpf et al., 2013). The above analysed processes are playing a role for the closure of cracks, as was showed in fig.7. In the present case study, we demonstrated how micro-scale infiltration can influence the degradation of surface of soil by inducing downward mass movements that are not reversible.

We have also shown here the great potential of high resolution three-dimensional point clouds of TLS or photogrammetry to analyse the processes that lead to erosion throughout surface mass movements at the millimetre scale. Investigations about erosion processes using point clouds are increasing in number. They use either Laser scanners for micro scale surface imaging (Schmid et al., 2004; Barneveld et al., 2013) or for cracks apertures (Sanchez et al., 2013). In addition, photogrammetry and especially Structure from Motion (SfM) are now being developed to analyse soil surface (Snapir et al., 2014).

This paper shows that monitoring the changes at millimetre scale to illustrate soil surface changes and erosion is now possible. This will help to design future experiments to analyse single processes such as swelling, crack closure, micro-landslides, and initiation of MDFs. With heavier rainfall those sediments will start to be mobilised on longer distances like MDFs and formation of rills. It shows also that material and rain intensity must be sufficient to permit an efficient detection of rain splash processes and associated erosion; more than 20 mm h^{-1} is necessary (Mathys et al., 2005).

Acknowledgements

Thanks to the *Observatoire de Recherche en Environnement* (ORE) of Draix, for letting us to sample soil into a protected area. Thanks are also due to the UNIBAT service of the University of Lausanne (UNIL), for providing meteorological data from their weather station. We thank also our colleagues Dr. M.-H. Derron, Benjamin Rudaz and Antonio Abellán for their comments and suggestions.

References

Antoine, P., Giraud, A., Meunier, M. and Van Asch, T.: Geological and geotechnical properties of the ‘terres noires’ in southeastern France: Weathering, erosion, solid transport and instability, Engineering Geology, 40, 223-234, 1995.

Barneveld, R.-J., Seeger, M. and Maalen-Johansen, I.: Assessment of terrestrial laser scanning technology for obtaining high-resolution DEMs of soils. Earth Surf. Process. Landforms, 38, 1096-9837, 2013.

Caris, J.P.T. and Van Asch, T.: Geophysical, geotechnical and hydrological investigations of a small landslide in the French Alps, Engineering Geology, 31, 249-276, 1991.

DeRose, R. C., Gomez B., Marden, M. and Trustrum, N. A.: Gully erosion in Mangatu Forest, New Zealand, estimated from digital elevation Models, Earth Surface Processes and Landforms, 23, 1045-1053, 1998.

Leica Geosystem AG: Leica ScanStation 2 technical note, Heerbrugg, Switzerland, Vl.07, 2007.

Malet, J.-P., Durand, Y., Remaître, A., Maquaire, O., Etchevers, P., Guyomarc’h, G., Déqué, M. and van Beek, L.P.H. Assessing the influence of climate change on the activity of landslides in the Ubaye Valley. In: McInnes, R., Jakeways, J., Fairbank, H., Mathie, E. (Eds): Proceedings of the International Conference on Landslides and Climate Change - Challenges and Solutions, Taylor & Francis, London, pp. 195-205, 2007.

Maquaire O., Ritzenthaler A., Fabre D., Ambroise B., Thiery Y., Truchet E., Truchet E., Malet J.-P. Caractérisation des profils de formations superficielles par pénétrometrie dynamique à énergie variable: application aux marnes noires de Draix (Alpes-de-Haute-Provence, France). Comptes Rendus Géosciences, 334, 835–841, 2002.

Mathys N., Klotz S., Esteves M., Descroix L. and Lapetite J.-M.: Runoff and erosion in the Black Marls of the French Alps: observations and measurements at the plot scale. Catena, 63, 261-281, 2005.

Mitchell AR AND van Genuchten MTh. Flood irrigation of a cracked soil. Soil Science Society of America Journal. 57, 490–497, 1993.

Oostwoud Wijdenes, D.J. and Ergezinger, P.: Erosion and sediment transport on steep marly hillslopes, Draix, Haute-Provence, France: an early experimental field study. Catena, 33, 179-200, 1998.

Sanchez M., Atique A., Kim S., Romero E. and Zielinski M. Exploring desiccation cracks in soils using a 2D profile laser device. Acta Geotechnica, 8, 583–596, 2013.

Schmid, T., Schack-Kirchner, H. and Hildebrand, E.: A Case Study of Terrestrial Laser-Scanning in Erosion Research: Calculation of Roughness Indices and Volume Balance at a Logged Forest Site. Eds: M. Thies, B. Koch, H. Spiecker and H. Weinacker: Laser-Scanners for Forest and Landscape Assessment. ISPRS Archives – V. XXXVI-8/W2 - WG VIII/2, 114-118, 2004.

Selby, M.J., Hillslope materials and processes: Oxford, UK, Oxford University Press, 252–258, 1993.

Shepard, D., A two dimensional interpolation function for irregularly-spaced data, New York, USA. Proceeding ACM '68 Proceedings of the 1968 23rd ACM national conference, 517-524 1968.

Snapir B., Hobbs S. and Waine T.W. Roughness measurements over an agricultural soil surface with Structure from Motion. ISPRS J. of Photogrammetry and Remote Sensing, 96, 210–223, 2014.

Stumpf, A., Malet, J.-P., Kerle, N., Niethammer, U., & Rothmund, S. Image-based mapping of surface fissures for the investigation of landslide dynamics. Geomorphology, 186, 12-27, 2013.

Torri, D., Regüés, D., Pellegrini, S. and Bazzoffi P.: Within-storm surface dynamics and erosive effects of rainstorms. Catena, 38, 131-150, 1999.

Table 1: Summary of the TLS scans table of the experiment for the TLS campaign of the 31st of June of 2010. This table compile the information concerning the scan time, the number of points before and after cleaning, the mean spacing between the points and the density of points.

Acquisition time	Number of points before cleaning	Mean spacing [mm]	Distance from TLS [m]	Number of points after cleaning	Density [pts/cm2]
11h01	601349	1	2	496391	84.84
12h00	149951	2	2	123233	21.06
14h00	149951	2	2	123477	21.10
14h30	149951	2	2	123269	21.07
15h00	149951	2	2	123496	21.11
15h30	149951	2	2	122857	21.00
16h00	149951	2	2	120162	20.54
16h30	149951	2	2	118301	20.22
17h00	149951	2	2	117290	20.05
17h30	149951	2	2	116322	19.88
17h32	601349	1	2	467484	79.90
17h47	601349	1	2	469906	80.31

Table 1: Recapitulative TLS scans table of the experiment (TLS campaign 31.05.2010), with for each scan its time, the number of points before and after cleaning, the mean spacing between the points and the density of points.

Acquisition time	Number of points before cleaning	Mean spacing [mm]	Distance from TLS [m]	Number of points after cleaning	Density [pts/cm2]
11h01	601349	1	2	496391	84.84
12h00	149951	2	2	123233	21.06
14h00	149951	2	2	123477	21.10
14h30	149951	2	2	123269	21.07
15h00	149951	2	2	123496	21.11
15h30	149951	2	2	122857	21.00
16h00	149951	2	2	120162	20.54
16h30	149951	2	2	118301	20.22
17h00	149951	2	2	117290	20.05
17h30	149951	2	2	116322	19.88
17h32	601349	1	2	467484	79.90
17h47	601349	1	2	469906	80.31

Figure 1: a. view of the sampling and the metal case (1 m x 0.5 m x 0.20 m) showing bottom plate partially entered and the approximate orientation of the bedding. b: View of the sample of soil inclined at 45° during the rainfall. c. Position of the TLS relatively to the metal case which is protected from rainfall by a tent.

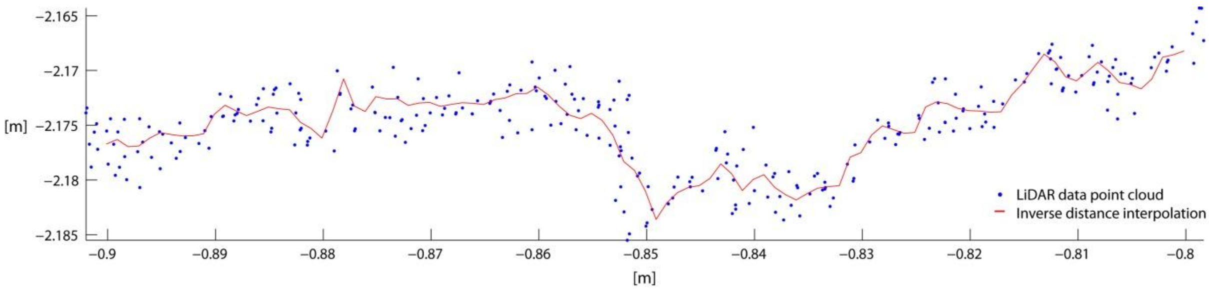

Figure 2: Downhill section of 10 cm long using the points over 1 cm width of the original TLS data point cloud compared with the 1 mm DEM profile (17h47 scan data). The profile has been performed with an inverse distance interpolation power one.

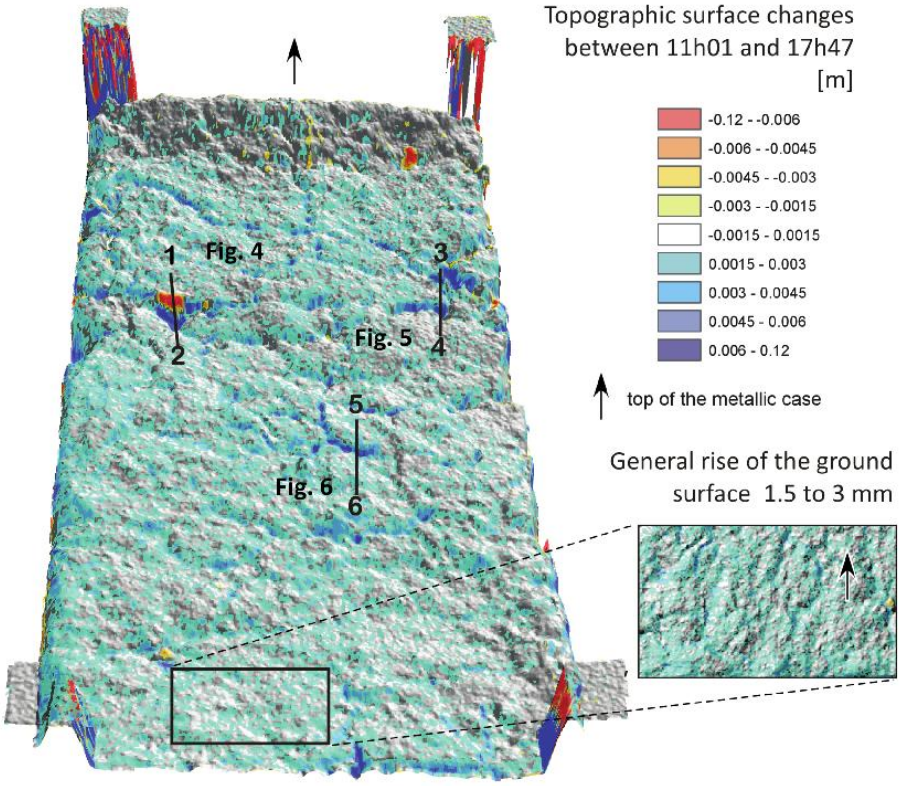

Figure 3: TLS scans comparison; topographic changes from 11h01 to 17h47 and surface detailed view. The locations of figures 4 to 6 are indicated.

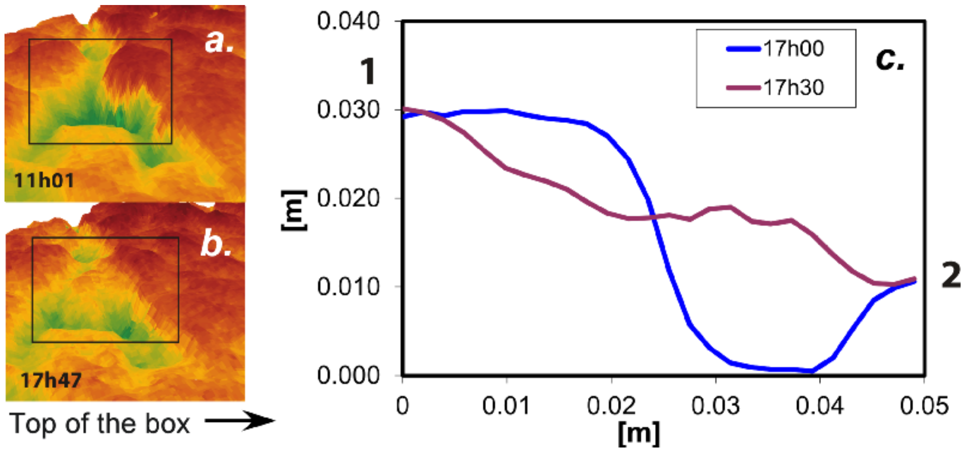

Figure 4: Profile changes showing a mass movement occurring between 17h00 and 17h30, but with the surface at 11h01 and 17h47. a. 3D view of the zone at 11h01 and b. at 17h47, the black box indicate the position of the profile c.

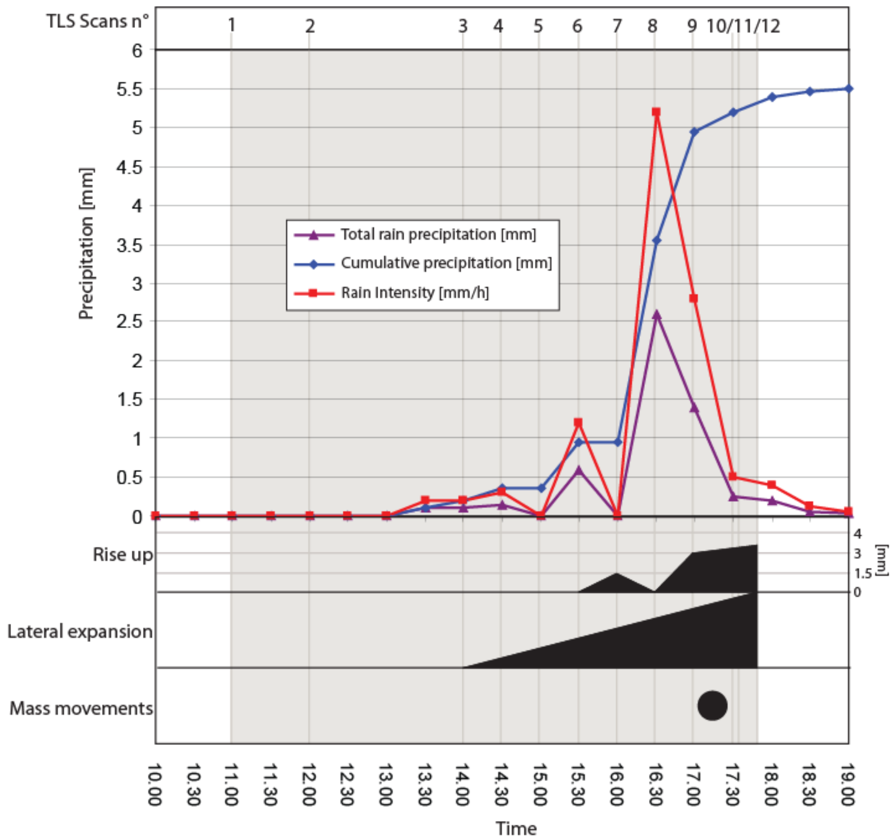

Figure 5: Observed phenomenon according to the precipitation data. The total rain amount in mm, the cumulative precipitation and the rain intensity are presented. The duration of the rising up is in mm, the lateral expansion with its intensity and mass movement processes are presented in relative scale.

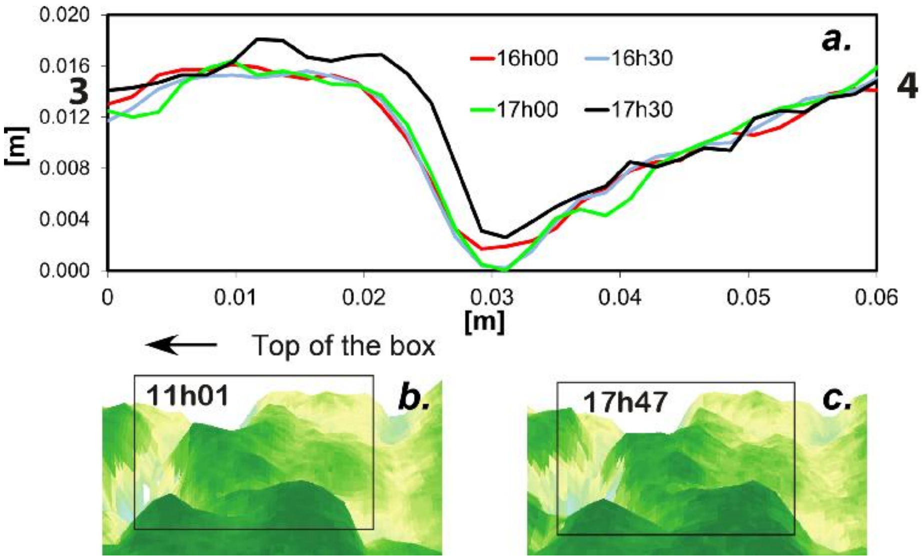

Figure 6: a. Profile changes showing evolution of lateral expansion and rise up from 16h00 and 17h30. b. 3D view of the zone at 11h01 and b. at 17h47, the black box indicate the position of the profile a.

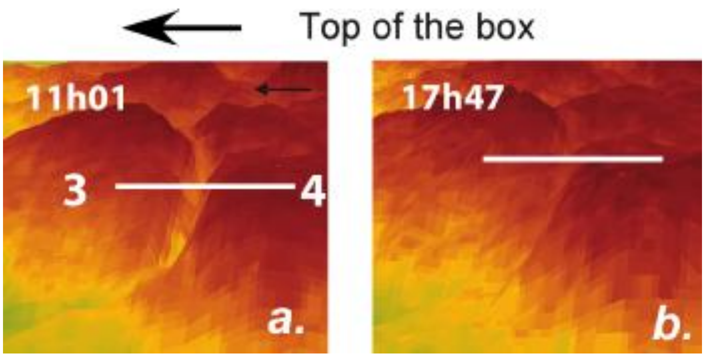

Figure 7: 3D views changes showing evolution of lateral expansion, showing a crack closure from 11h01 (a) to 17h47 (b).